J Electroceram (2010) 24:231–236
DOI 10.1007/s10832-009-9563-1

Influence of the processing rates and sintering temperatures on the dielectric properties of $CaCu_3Ti_4O_{12}$ ceramics

Seunghwa Kwon · David P. Cann

Received: 13 July 2008 / Accepted: 13 January 2009 / Published online: 28 January 2009

Abstract The stoichiometric $CaCu_3Ti_4O_{12}$ pellets were prepared by the solid state synthesis. X-ray diffraction data revealed the tenorite CuO and cuprite Cu_2O secondary phases on the unpolished $CaCu_3Ti_4O_{12}$ samples regardless of the heating rates. Also, the dielectric constant marked the highest for the $CaCu_3Ti_4O_{12}$ sample sintered at the lowest heating rate (1°C/min), which was explained by the increased grain conductivity due to the cation reactions. On the other hand, Cu_2O phase was found only on the unpolished $CaCu_3Ti_4O_{12}$ sample sintered over 1100°C and those are considered as the remains reduced from the CuO phase. The higher sintering temperature showed the increased dielectric constant and the loss tangent of the $CaCu_3Ti_4O_{12}$ samples, and this result could be interpreted by the impedance measurement data. The relationship between the processing condition and the dielectric properties was discussed in terms of the cation non-stoichiometry and the defect chemistry in $CaCu_3Ti_4O_{12}$.

Keywords Ceramic processing · Dielectric properties · Cation stoichiometry · Defects

1 Introduction

From ongoing technological trends of miniaturization, the demand for temperature-stable high permittivity capacitors has increased. Recent examples of these capacitors include fuel cell systems with ultracapacitors in hybrid-electric vehicles [1], pulsed power systems such as electrothermal and electromagnetic weapons systems [2], and many others. Since the relative permittivity (ε_r') is the key parameter in the performance of the materials, there has been a great deal of attention in high-K dielectrics. The most common materials exhibiting giant dielectric constants are either Perovskite-based ferroelectric ceramics such as $BaTiO_3$ with its solid solution members (e.g. $BaTiO_3$ and $MgSnO_3$, $BaTiO_3$ with $SrTiO_3$ and $CaTiO_3$, etc) [3] or the relaxor ferroelectrics including $Pb(Mg_{1/3}Nb_{2/3})O_3$, $Pb(Zn_{1/3}Nb_{2/3})O_3$, and $Pb_{1-x}La_x(Zr_{1-y}Ti_y)O_3$ [4]. However, these compounds often present strong temperature dependence due to structural transitions which are undesirable for most applications. From this point of view, the unusual properties in the high-K material $CaCu_3Ti_4O_{12}$ (CCTO, hereafter), discovered by Subramanian et al. [5], has been the focus of many researchers. The dielectric constant of CCTO maintains over 10^4 at room temperature, but it is temperature independent over the temperature range of 100–400 K as well [6]. Throughout many attempts to elucidate the origin of this unusual behavior of CCTO, the extrinsic models were supported by the evidence of twin boundaries in single crystal CCTO [7] as well as domain boundaries in polycrystalline CCTO [8]. Based on the Maxwell–Wagner model [9–11], an electrically heterogeneous structure in polycrystalline CCTO creates polarization due to the presence of mobile charged species and internal interfaces. In CCTO, this heterogeneity has been represented by conducting grains and insulating boundaries and has been widely attributed to the internal barrier layer capacitor model [12].

It has been previously reported that the dielectric properties of CCTO are largely influenced by factors such as doping schemes [13–16] as well as stoichiometric variations [17–19]. However, it seems that both the

S. Kwon (✉) · D. P. Cann
Materials Science, School of Mechanical, Industrial,
and Manufacturing Engineering, Oregon State University,
204 Rogers Hall,
Corvallis, OR 97331, USA
e-mail: kwonse@onid.orst.edu

dielectric constant and loss tangent values of CCTO are strongly dependent upon the processing conditions. Recent publications confirmed the sensitivity of the dielectric properties by means of a variety of different processes such as different calcination temperatures [20], sintering times [21], and sintering temperatures [22]. In this work, the effects of processing rates on the dielectric properties of CCTO are investigated by controlling the heating and cooling rates during the sintering. Also, the dielectric constant and loss tangent versus frequency were measured and compared with the stoichiometric CCTO ceramics that were sintered at different temperatures.

2 Experimental

The stoichiometric $CaCu_3Ti_4O_{12}$ ceramics were prepared via a conventional solid state method. Each reactant powder of highly pure (>99.9%) $CaCO_3$, CuO, and TiO_2 was mixed and milled in ethanol with Y_2O_3-stabilized ZrO_2 media by using a vibratory mill (SWECO, Florence, KY). Then, the mixed powders were calcined at 1000°C in air for 24 h. The homogeneous CCTO powder could be confirmed through x-ray diffraction (XRD). Following the second milling of the calcined powders, green pellets of CCTO (diameter of 12.7 mm) were produced by using a cold uniaxial press (Carver Press Inc.) with approximately 3 wt.% of organic binder. In order to study the different sintering effects, first group of green CCTO pellets were sintered up to 1100°C in air for 2 h with the different heating rates (1, 5, and 10°C/min) followed by a variety of cooling rates (1, 5, 10°C/min, and air quenching). On the other hand, green CCTO samples from the second group were sintered at the different temperatures such as 1050, 1075, 1100, and 1115°C for 2 h with the heating rate of 5°C/min and quenched in air. Both surface (unpolished) and inner layer (polished, ~80% of the original thickness) of the CCTO pellets under the various sintering conditions were examined via an X-ray diffractometer (Bruker D8 Discover) for the phase stability. Density of the polished CCTO samples was measured by using the Archimedes method. Each sample representing the distinct sintering process was coated with gold through a sputtering unit, and the dielectric constant and the loss tangent were measured in terms of the frequency $f=10^2$–10^6 Hz with an Agilent 4284A LCR meter at room temperature. In addition, an HP 4194A impedance analyzer was utilized to measure the bulk and boundary resistivity from 10 Hz to 5 MHz.

3 Results and discussion

A plot of the X-ray diffraction patterns of unpolished CCTO samples after quenching is shown in Fig. 1. Regardless of the heating rates (1, 5 and 10°C/min), all three XRD patterns were matched with the major peaks of the pseudo-cubic CCTO provided by the Powder Diffraction File database (PDF 75-2188) except for two minor peaks that are clearly seen in the inset of Fig. 1. These small peaks appeared around 35.5° and 38.8° and can be attributed to tenorite CuO. Another peak near 36.5° can be attributed to a cuprite Cu_2O phase. To further examine these secondary peaks, the intensity ratios of CuO and Cu_2O to the CCTO peak at the maximum (2θ~34.3°) were calculated. As seen in Table 1, the ratio of CuO to CCTO peak (I_{CuO}/I_{CCTO}) marked the lowest value at the heating rate of 5°C/min (H05, hereafter) while the value increases at 1 and 10°C/min (hereafter H01 and H10, respectively). In addition, the calculated Cu_2O/CCTO ratio for those samples increased with increasing heating rates. On the other hand, the XRD patterns of the polished samples (not shown) showed that only peaks due to Cu_2O were present, which provides evidence of the limited reoxidation of inner layer regardless of the heating rates. Like the case of I_{CuO}/I_{CCTO}, the calculated lattice parameters showed no obvious correlation to the heating rate. This is likely due to the complex changes in cation stoichiometry in CCTO caused by the reduction/reoxidation process and intrinsic Cu volatility, which eventually leads to dynamic changes in Cu and O content.

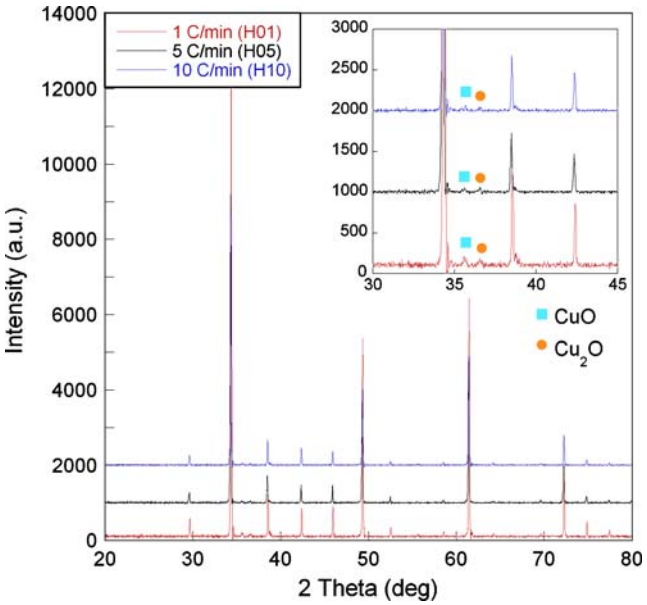

Fig. 1 XRD patterns of the CCTO samples (unpolished) sintered at the different heating rates

To further examine the effects of heating rate on the properties of CCTO, the dielectric constant and the loss tangent were measured as a function of frequency and are plotted in Fig. 2(a). It is clear that the dielectric constant of CCTO increased as the sintering rate was reduced over the entire range of frequency. At 1 kHz, a K~15,900 was measured for the H01 sample while the dielectric constants

Table 1 Intensity ratios and lattice parameter of CCTO with different heating rates.

	Heating rates		
	1°C/min	5°C/min	10°C/min
I_{CuO}/I_{CCTO} (unpolished)	0.0187	0.0131	0.0185
I_{Cu2O}/I_{CCTO} (unpolished)	0.0055	0.0070	0.0073
I_{Cu2O}/I_{CCTO} (polished)	0.0106	0.0159	0.0132
Lattice parameter (Å)	7.3832	7.3912	7.3886

of H05 and H10 samples were about 12,700 and 11,800, respectively. The loss tangent of the H01, H05, and H10 CCTO samples is shown in Fig. 2(b). Like the dielectric constant, tan δ follows the analogous pattern of changes with regard to the heating rates over the measured frequencies though there was negligible difference in tan δ between 1–10 kHz. The enhancement in dielectric constant at a low heating rate can be explained through the changes in cation stoichiometry that occurred during the sintering process. First proposed by Li et al. [23], at high temperatures divalent Cu ions are reduced to the monovalent state and in addition there is a substitution of tetravalent Ti ions into the Cu sites to maintain charge compensation during the heating. Upon cooling, these Cu^{1+} ions are reoxidized to Cu^{2+} where the electrons move into the Ti 3d conduction band and this results in an observed increase in conductivity. It is expected that the slower heating rates (e.g. H1) would allow sufficient kinetics to create a higher concentration of Cu^{1+} and eventually an enhanced conductivity after cooling. Assuming negligible cation migration during the rapid cooling, the higher dielectric constants observed can be explained by an increase in the grain conductivity of the H1 sample. Even though Wang et al. [24] suggested the possibility of the migration of Ti ions into the boundaries, it seems that nearly constant values of loss tangent at frequencies below 10 kHz independent of the heating rates support the suggestion of limited cation migration after quenching. Lastly, the increased dielectric constant [Fig. 3(a)] and tan δ [below 10 kHz, Fig. 3(b)] of the CCTO sample sintered at the slower cooling rate (under a fixed heating rate of 5°C/min) clearly indicates increased grain conductivity as a result of the increased Cu non-stoichiometry due to reoxidation processes. This is also consistent with the observed shift of the shoulder of the relaxation frequency near 1 MHz in the tan δ data.

The XRD patterns of the unpolished CCTO samples sintered at 1050, 1075, 1100, and 1115°C for 2 h (hereafter 1050–2 h, 1075–2 h, 1100–2 h, 1115–2 h, respectively) were plotted in Fig. 4(a). From the enlarged patterns between 30 and 50° of 2-theta shown in Fig. 4(b), two CuO peaks were found in all CCTO samples regardless of the sintering temperatures. However, Cu_2O peaks could only be observed in the samples sintered at the two highest temperatures (i.e. 1100–2 h and 1115–2 h). Based on the Cu–O Richardson diagram [25], the phase transition between CuO and Cu_2O is expressed by the following chemical equation:

$$Cu_2O(s) + {}^1\!/_2\, O_2(g) \Leftrightarrow 2CuO(s) \quad (1)$$

The transition temperatures between these phases are dependent upon the oxygen partial pressure, and as Li et al. [26] mentioned, CuO is reduced to Cu_2O around T= 1300 K in air (i.e. $pO_2 \sim 0.21$). While Cu_2O peaks were

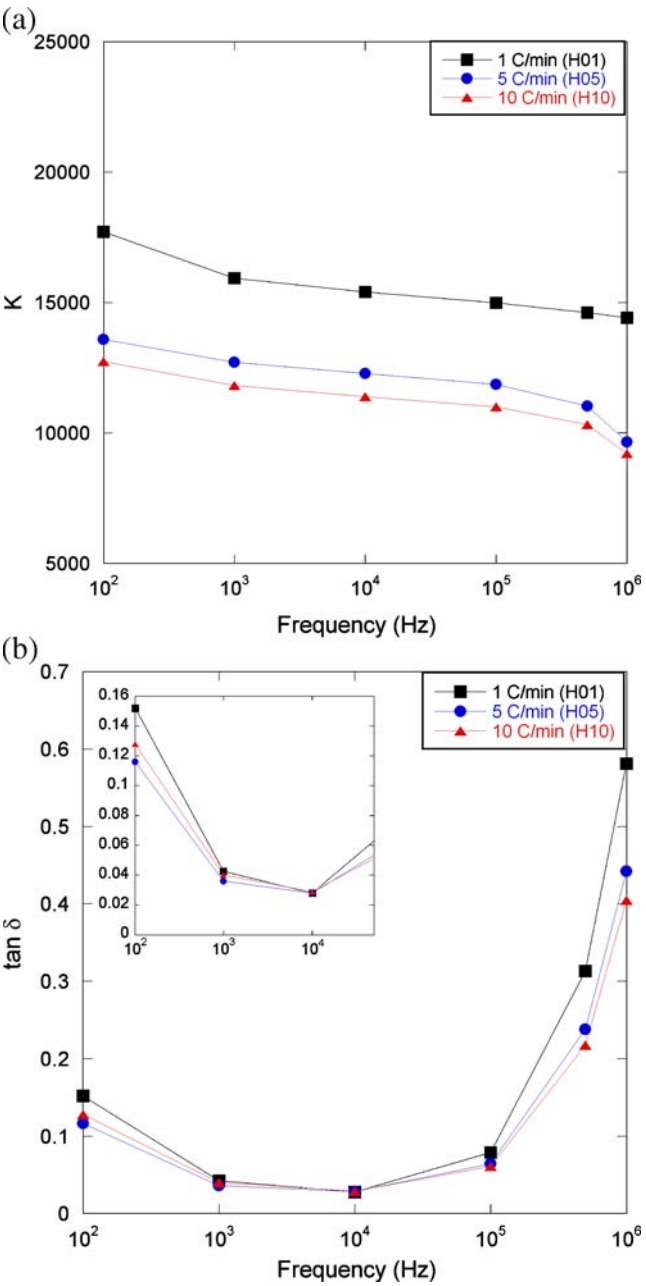

Fig. 2 Plots of the (**a**) dielectric constant and (**b**) loss tangent versus frequency of the CCTO samples (polished) in terms of the heating rates

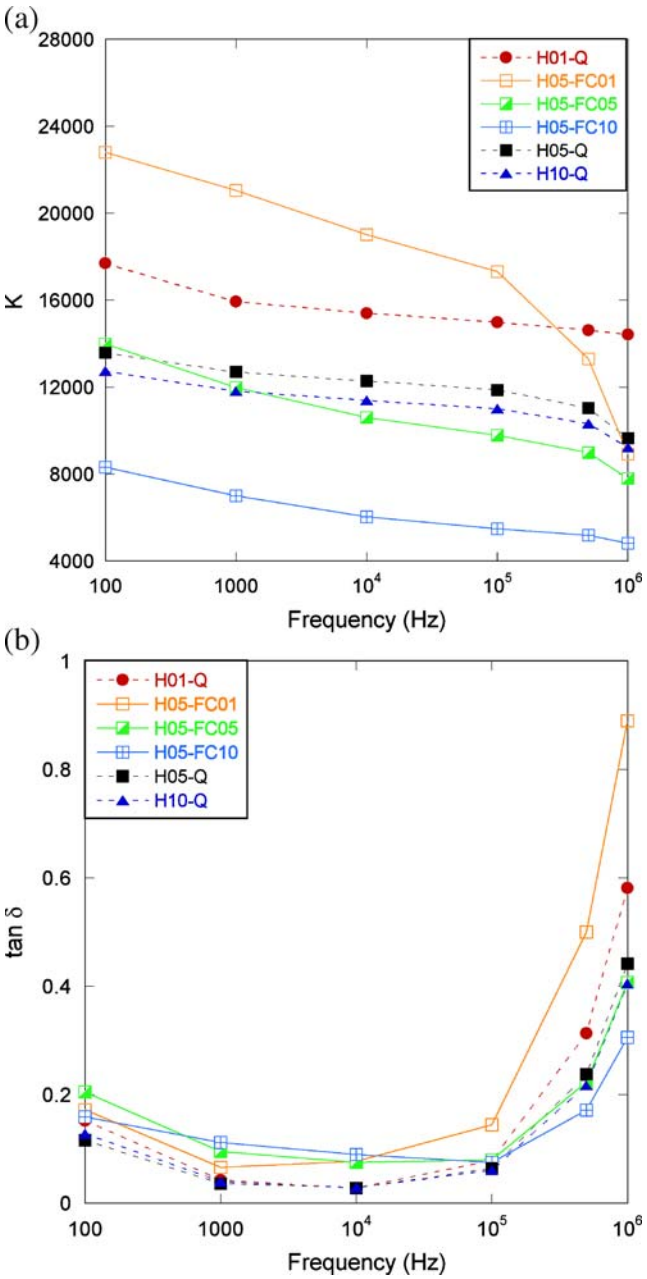

Fig. 3 Plots of the (**a**) dielectric constant and (**b**) tan δ versus frequency of the polished CCTO samples sintered at the various heating and cooling rates

absent in the XRD data for the 1050–2 h and 1075–2 h samples, the presence of both CuO and Cu_2O in both 1100–2 h and 1115–2 h samples indicate that Cu_2O is formed according to Eq. 1 above. Furthermore, the Cu_2O phase partially transformed to CuO upon cooling through a reoxidation process near the surface of the ceramic. In contrast to the unpolished CCTO, the XRD patterns of the polished samples (not shown here) exhibit only peaks arising from Cu_2O (2θ~36.5°) regardless of the sintering temperatures. This is indicative of limited oxygen diffusion in the interior of the sample which prevents the reoxidation of Cu_2O to CuO.

In Fig. 5(a), the dielectric constant of the 1050–2 h, 1075–2 h, 1100–2 h, and 1115–2 h CCTO samples is plotted as a function of frequency. It is clear that the dielectric constant rises by increasing the sintering temperature. Unlike the relatively low dielectric constants of 1050–2 h (3900 at 10 kHz) and 1075–2 h samples (5100 at 10 kHz), sintering at 1100°C and above resulted in a significant increase in the dielectric constant as large as 25,100 (f=10 kHz) for the CCTO sample sintered at 1115°C. On the other hand, the loss tangent of these samples follows the analogous trend of the dielectric constant. As seen in

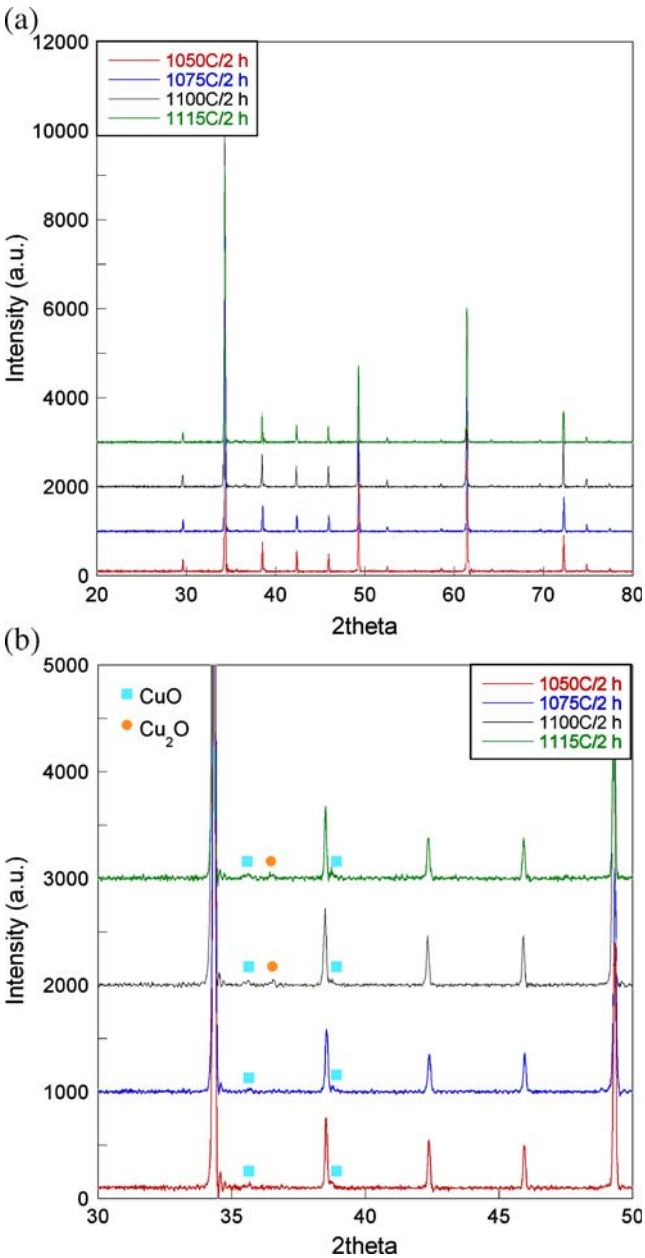

Fig. 4 XRD patterns of the unpolished CCTO samples sintered at the different temperatures with (**a**) overall (20–80°) and (**b**) zoom-in (30–45°) range of 2-theta

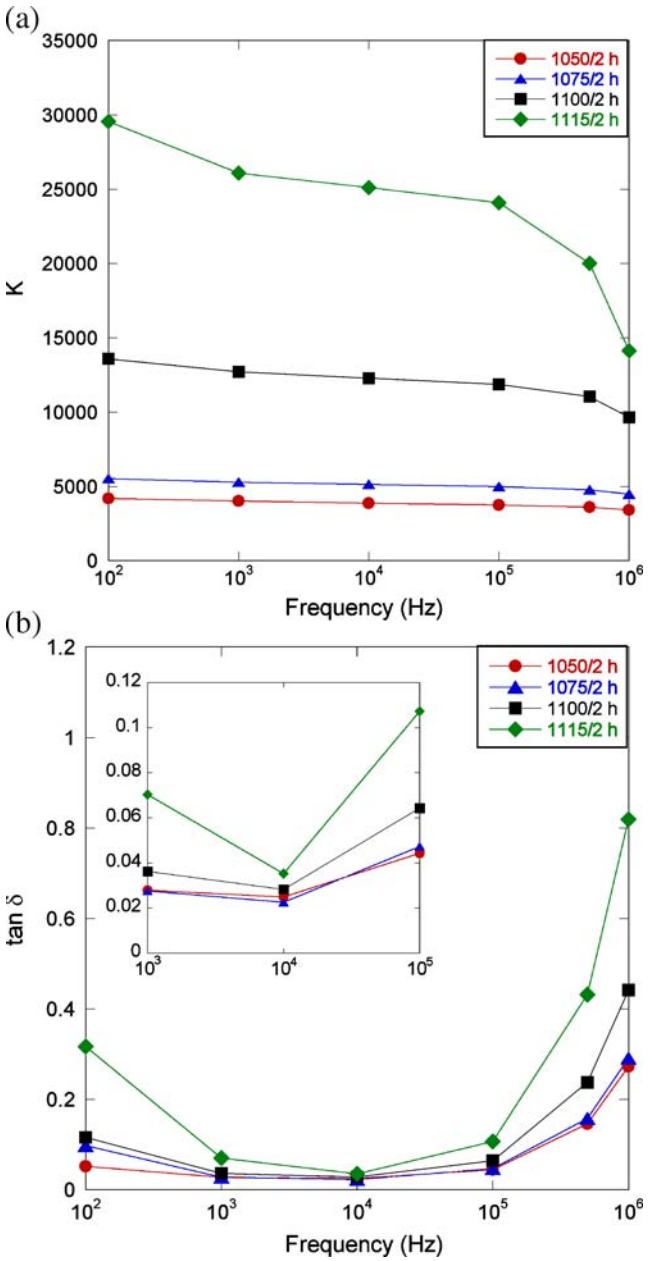

Fig. 5 Frequency dependence of the (**a**) dielectric constant and (**b**) tan δ of the polished CCTO samples sintered at the various temperatures

Fig. 5(b), tan δ increases with the sintering temperature. At 10 kHz, tan δ of 1115–2 h sample was 0.035 while the lowest loss was marked as 0.022 from 1075–2 h sample [shown in the inset of Fig. 5(b)]. These dielectric properties provided by the different sintering temperatures can be further discussed via impedance spectroscopy. Based on the internal barrier layer capacitor model proposed by Sinclair et al. [27], both grain and boundary resistivity can be determined by using the two equivalent parallel circuits indicating the grain and boundary component. The complex impedance plane plots of CCTO sintered at for different temperatures are shown in Fig. 6(a). Also, curve fittings of these impedance data are given in Fig. 6(b). It is clearly seen that curve fittings are well matched with the measured data. By using the measured impedance data and dimensions of CCTO samples, the grain resistivities of 1050–2 h, 1075–2 h, 1100–2 h, and 1115–2 h CCTO were obtained as 116.2, 91.8, 67.0, and 54.8 Ω cm, respectively at high frequency, while their boundary (or bulk) resistivities were 2.35×10^{8}, 6.52×10^{7}, 6.23×10^{7}, and 5.22×10^{6} Ω cm at low frequency. That is, the highest dielectric constant and loss tangent observed from the 1115–2 h sample can be interpreted by its relatively high grain conductivity but also the lowest resistivity of its boundary regions. Li et al. [23] reported the similar result such that the largest dielectric constant was obtained from CCTO crystals of the melt that are processed at the maximum possible sintering temperature, and they explained this improved dielectric constant as more con-

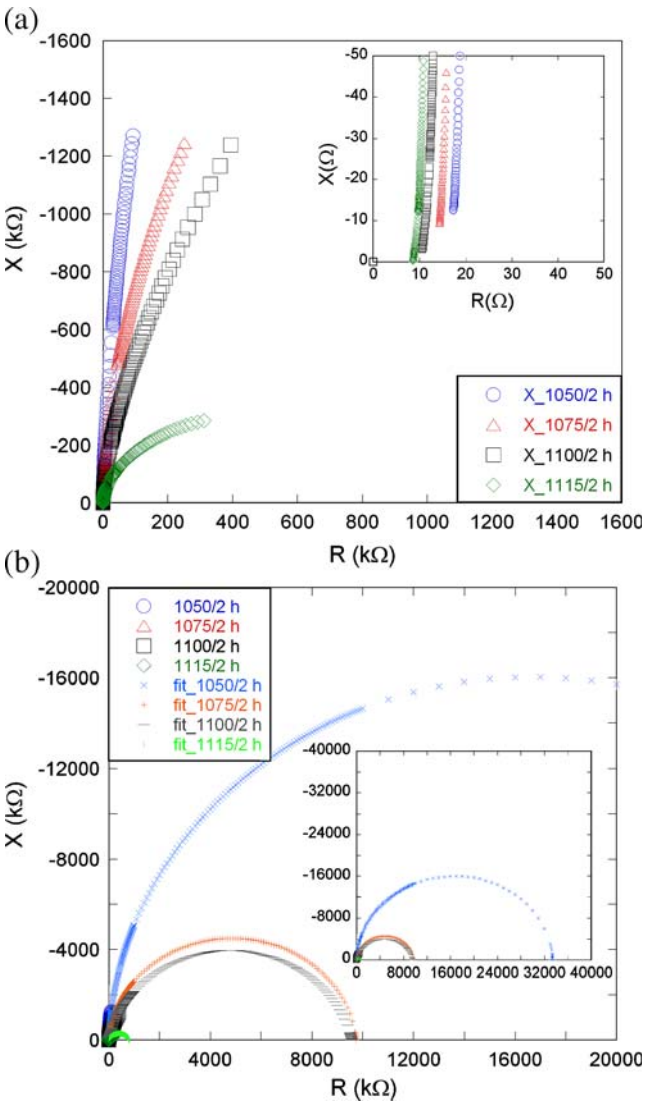

Fig. 6 (**a**) Impedance complex plane plots and (**b**) their fitting curves of the polished CCTO samples sintered at the different temperatures

ducting CCTO due to the higher value of x in CCTO (i.e. Cu_{1-x}^{2+}). Based on our previous report [28] of Cu volatility occurred over its melting temperature of 1084.6°C [29], the larger Cu volatility in CCTO at the higher sintering temperature might be responsible for the increased dielectric constant indicated by the lower bulk resistivity of CCTO samples. The evidence of the non-stoichiometric CCTO has been previously reported [17, 30–31], but the further investigation of its defect chemistry is necessary and this might provide the clues for the better understanding of the property-structure relationship in CCTO ceramics.

4 Conclusion

From X-ray diffraction data, CuO and Cu_2O phases were found on the surface of CCTO ceramics with intensity ratios that depended on the heating rate. An increase in the dielectric constant was observed at the lowest heating rate that can be attributed to an increase in the grain conductivity due to changes in the cation stoichiometry in the CCTO phase (i.e. copper and titanium ions). In addition, relatively constant values of tan δ between 1–10 kHz might indicate the limited cation migration into the boundary regions upon rapid cooling. The effects of the sintering temperature on the dielectric properties were also investigated and the CCTO samples sintered at $T \geq 1100$°C indicated a marked increase in dielectric constant compared to the ceramics sintered below 1075°C. With supportive evidence of a Cu_2O phase revealed through the diffraction patterns as well as the grain and boundary resistivity obtained via impedance measurements, the increase in both dielectric constant and loss tangent in the CCTO samples sintered at higher temperatures (T=1100°C and 1115°C) can be explained by cation non-stoichiometry caused by reduction/oxidation reactions and Cu volatility.

Acknowledgements This work was supported by the Office of Naval Research Capacitor Program and the American Chemical Society's Petroleum Research Foundation.

References

1. G. Zorpette, IEEE Spectrum **42**, 32 (2005). doi:10.1109/MSPEC.2005.1377872
2. D.-Y. Jeong, S.-J. Yoon, Electron. Mater. Lett. **2**(3), 207 (2006)
3. C. Relva, Buchanan (ed.), *Ceramic Materials for Electronics: Processing, Properties, and Applications, 2nd edn.* (Marcel Dekker, New York, 1991), p. 79
4. A.J. Moulson, J.M. Herbert, *Electroceramics*, 2nd edn. (Wiley, Chichester, 2003), p. 320
5. M.A. Subramanian, D. Li, N. Duan, B.A. Reisner, A.W. Sleight, J. Solid State Chem. **151**, 323 (2000). doi:10.1006/jssc.2000.8703
6. A.P. Ramirez, M.A. Subramanian, M. Gardel, G. Blumberg, D. Li, T. Vogt, S.M. Shapiro, Solid State Commun. **115**, 217 (2000). doi:10.1016/S0038-1098(00)00182-4
7. M.A. Subramanian, A.W. Sleight, Solid State Sci. **4**, 347 (2003). doi:10.1016/S1293-2558(01)01262-6
8. T.-T. Fang, C.-P. Liu, Chem. Mater. **17**, 5167 (2004). doi:10.1021/cm051180k
9. P. Lunkenheimer, V. Bobnar, A.V. Pronin, A.I. Ritus, A.A. Volkov, A. Loidl, Phys. Rev. B **66**, 052105 (2002). doi:10.1103/PhysRevB.66.052105
10. J. Volger, ed. by A.F. Gibson. *rogress in Semiconductors, Vol. 4* (Wiley, New York, 1960), p. 207
11. S. Aygün, X. Tan, J.-P. Maria, D.P. Cann, J. Electroceram. **15**(3), 203 (2005). doi:10.1007/s10832-005-3191-1
12. T.B. Adams, D.C. Sinclair, A.R. West, Adv. Mater. **14**(18), 1321 (2002). doi:10.1002/1521-4095(20020916)14:18<1321::AID-ADMA13217>3.0.CO;2-P
13. W. Kobayashi, I. Terasaki, Physica B **329-333**, 771 (2003). doi:10.1016/S0921-4526(02)02517-6
14. G. Chiodelli, V. Massarotti, D. Capsoni, M. Bini, C.B. Azzoni, M. C. Mozzati, P. Lupotto, Solid State Commun. **132**, 241 (2004). doi:10.1016/j.ssc.2004.07.058
15. S.-Y. Chung, S.-Y. Choi, T. Yamamoto, Y. Ikuhara, S.-J.L. Kang, Appl. Phys. Lett. **88**, 091917 (2006). doi:10.1063/1.2179110
16. S. Kwon, C.-C. Huang, E.A. Patterson, E.F. Alberta, S. Kwon, W. S. Hackenberger, D.P. Cann, Mater. Lett. **62**, 633 (2008). doi:10.1016/j.matlet.2007.06.042
17. T.-T. Fang, L.-T. Mei, H.-F. Ho, Acta Mater. **54**, 2867 (2006). doi:10.1016/j.actamat.2006.02.037
18. K. Chen, Y.F. Liu, F. Gao, Z.L. Du, J.M. Liu, X.N. Ying, X.M. Lu, J.S. Zhu, Solid State Commun. **141**, 440 (2007). doi:10.1016/j.ssc.2006.12.004
19. S.F. Shao, J.L. Zhang, P. Zheng, C.L. Wang, Solid State Commun. **142**, 28 (2007). doi:10.1016/j.ssc.2007.02.025
20. B.A. Bender, M.-J. Pan, Mater. Sci. Eng. B **117**, 339 (2005). doi:10.1016/j.mseb.2004.11.019
21. B. Shri Prakash, K.B.R. Varma, Physica B **382**, 312 (2006). doi:10.1016/j.physb.2006.03.005
22. R. Aoyagi, M. Iwata, M. Maeda, Ferroelectrics **356**, 90 (2007). doi:10.1080/00150190701509306
23. J. Li, M.A. Subramanian, H.D. Rosenfeld, C.Y. Jones, B.H. Toby, A.W. Sleight, Chem. Mater. **16**, 5223 (2004). doi:10.1021/cm048345u
24. C. Wang, H.J. Zhang, P.M. He, G.H. Cao, Appl. Phys. Lett. **91**, 052910 (2007). doi:10.1063/1.2768006
25. O. Kubaschewski, C.B. Alcock, P.J. Spencer, Materials Thermochemistry, 6th edn. (Pergamon, New York, 1993)
26. J. Li, A.W. Sleight, M.A. Subramanian, Solid State Commun. **135**, 260 (2005). doi:10.1016/j.ssc.2005.04.028
27. D.C. Sinclair, T.B. Adams, F.D. Morrison, A.R. West, Appl. Phys. Lett. **80**(12), 2153 (2002). doi:10.1063/1.1463211
28. S. Kwon, N. Triamnak, D.P. Cann, Proceedings of the 17th International Symposium on Applications of Ferroelectrics, Santa Fe, NM, (2008). doi:10.1109/ISAF.2008.4688095
29. Oregon State University online network. http://www.webelements.com/webelements/element/text/Cu/heat.html. Accessed on June 15, 2008
30. T.B. Adams, D.C. Sinclair, A.R. West, J. Am. Ceram. Soc. **89**(9), 2833 (2006)
31. S. Kwon, C.-C. Huang, M.A. Subramanian, D.P. Cann. J. Alloy. Comp., in press (2009). doi:10.1016/j.jallcom.2008.06.015